Received 14 August 2023; revised 6 February 2024 and 11 March 2024; accepted 11 March 2024. Date of publication 25 March 2024; date of current version 23 April 2024. The review of this article was arranged by Editor Paolo Bonato.

Digital Object Identifier 10.1109/OJEMB.2024.3381475

An Investigation of Manifold-Based Direct Control for a Brain-to-Body Neural Bypass

E. LOSANNO [1,2], M. BADI [3], E. ROUSSINOVA [3], A. BOGAARD [4], M. DELACOMBAZ[4], S. SHOKUR [3] (Senior Member, IEEE), AND S. MICERA [1,2,3] (Fellow, IEEE)

[1]The Biorobotics Institute and Department of Excellence in Robotics and AI, Scuola Superiore Sant'Anna, 56025 Pisa, Italy
[2]Modular Implantable Neuroprostheses (MINE) Laboratory, Università Vita-Salute San Raffaele and Scuola Superiore Sant'Anna, Milan, Italy
[3]Bertarelli Foundation Chair in Translational Neuroengineering, Center for Neuroprosthetics and Institute of Bioengineering, École Polytechnique Fédérale de Lausanne (EPFL), 1015 Lausanne, Switzerland
[4]Department of Neuroscience and Movement Sciences, Platform of Translational Neurosciences, Section of Medicine, Faculty of Sciences and Medicine, University of Fribourg, 1700 Fribourg, Switzerland

CORRESPONDING AUTHOR: S. Micera (e-mail: silvestro.micera@epfl.ch).

This work was supported by the Swiss National Science Foundation grant Neugrasp under Grant 205321_170032, in part by the Wyss Center for Bio and Neuroengineering, and in part by the Bertarelli Foundation. *(S. Shokur and S. Micera contributed equally to this work.)*
This article has supplementary downloadable material available at https://doi.org/10.1109/OJEMB.2024.3381475, provided by the authors.

ABSTRACT *Objective:* Brain-body interfaces (BBIs) have emerged as a very promising solution for restoring voluntary hand control in people with upper-limb paralysis. The BBI module decoding motor commands from brain signals should provide the user with intuitive, accurate, and stable control. Here, we present a preliminary investigation in a monkey of a brain decoding strategy based on the direct coupling between the activity of intrinsic neural ensembles and output variables, aiming at achieving ease of learning and long-term robustness. *Results:* We identified an intrinsic low-dimensional space (called manifold) capturing the co-variation patterns of the monkey's neural activity associated to reach-to-grasp movements. We then tested the animal's ability to directly control a computer cursor using cortical activation along the manifold axes. By daily recalibrating only scaling factors, we achieved rapid learning and stable high performance in simple, incremental 2D tasks over more than 12 weeks of experiments. Finally, we showed that this brain decoding strategy can be effectively coupled to peripheral nerve stimulation to trigger voluntary hand movements. *Conclusions:* These results represent a proof of concept of manifold-based direct control for BBI applications.

INDEX TERMS Brain-body interfaces, direct control, hand movement control, neural manifold, peripheral neurostimulation.

IMPACT STATEMENT This work shows that a brain decoding paradigm based on the direct link between intrinsic neural ensemble dynamics and output commands can provide intuitiveness and stability and can be effectively integrated with peripheral nerve stimulation for voluntary hand control.

I. INTRODUCTION

Brain-body interfaces (BBIs) are neuroprostheses that allow users to voluntarily control the movement of their body through an artificial neural bypass. A survey of patients with tetraplegia due to spinal cord injury [1] showed that BBIs are the preferred solution compared to the control of external robotic devices characterizing classic brain-machine interfaces (BMIs) [2]. In BBIs, brain activity recorded from motor cortical areas using invasive [3], [4], [5], [6], [7], [8], [9], [10] or non-invasive [11], [12] interfaces is translated into motion commands to actuate limbs via electrical stimulation of neuromuscular structures. Thus, BBIs need to tackle two complex neurotechnological modules, i.e., a motor decoding module and a movement restoration module, and their integration [13].

Focusing on the restoration of hand function, an ideal BBI should effectively integrate an easy-to-learn, accurate, and stable brain decoding paradigm with a motor restoration

module allowing the selective control of the hand. Recently, we demonstrated in a preclinical study in monkeys that peripheral nerve stimulation (PNS) at the intrafascicular level can evoke multiple grasps and hand extension movements with only two nerve implants [14], thus complying with the requirement of movement selectivity. Here, we present a brain decoding module based on the direct linear coupling between intrinsic neural ensemble dynamics and motion commands, aiming at achieving ease of learning and temporal stability.

To design our brain decoding strategy, we built on neuroscience studies [15], [16], [17] showing that neural population dynamics is constrained by the brain circuitry in a low-dimensional space, i.e., the neural manifold, spanned by the so-called neural modes, and that learning a new task is facilitated when the underlying neural activity pattern lies within this intrinsic manifold [17]. Moreover, it has been demonstrated that low-dimensional dynamics associated to movement remain stable over long periods of time [18]. Based on these findings, we hypothesized that by directly linking the activation of intrinsic neural modes to the controlled variables, the subject could intuitively learn to modulate this activation in such a manner that compensates for recording instabilities. Thus, we extended the previously validated approach of direct control based on the voluntary modulation of single-neuron activity aided by biofeedback [3] to the use of intrinsic neural ensemble dynamics.

We preliminarily examined the performance of the manifold-based direct control strategy in a macaque monkey. Specifically, we computed a 2D manifold capturing a significant portion of the variance of the animal's neural activity while performing a behavioral grasping task. We then coupled the activation of the two fixed neural modes to the 2D movement of a cursor and tested this BMI paradigm in a simple point-to-point task with incremental variations over weeks. This BMI phase was used to evaluate the intuitiveness and long-term performance of our decoding strategy. We show that, by daily recalibrating only global decoding scale factors, the monkey could succeed rapidly and robustly over time. Finally, we additionally coupled the dynamics of the two neural modes to the amplitude of stimuli delivered by intrafascicular electrodes implanted in the animal's arm nerves. We demonstrate that our decoding strategy is not affected by intrafascicular neuromodulation. Therefore, it can be used in a BBI exploiting intrafascicular PNS to trigger voluntary hand movements.

II. RESULTS

We tested a manifold-based direct control paradigm to control two degrees of freedom (DoFs) in a macaque monkey implanted with a 48-channel intracortical array in the hand region of primary motor cortex (M1). We distinguish three phases of the experimental protocol: (i) a control space construction phase, in which the 2D neural manifold was identified, (ii) a BMI phase, in which the monkey used the activation of the neural modes spanning the manifold found in (i) to directly control a cursor on a screen, and (iii) a BBI phase in which the monkey used the same manifold-based direct control strategy to actuate the hand via intrafascicular PNS.

A. CONSTRUCTION OF A 2D BRAIN CONTROL SPACE BASED ON MOTOR NEURAL MODES

We identified an intrinsic 2D neural manifold associated with a hand motor task as the brain control space for direct control of 2 DoF cursor and hand movements. During the dedicated session, we recorded M1 activity of the monkey while performing center-out reaching and grasping of objects mounted on a robotic arm [19] (Fig. 1(a)). Using principal component analysis (PCA) [15], we derived the first three PCs, i.e., the directions of highest variance, of the recorded M1 activity, representing the first three neural modes. The three PCs explained 13%, 8%, and 5% of total variance, respectively. We then examined the dynamics of the three so-called latent variables [15], computed by projecting M1 activity along the three neural modes, during the motor task to select the two control signals for the subsequent direct control experiments. We relied on the hypothesis that the two intrinsically most modulated latent variables would provide a larger working range when directly coupled to output commands. A higher modulation depth (i.e., difference between maximum and minimum values during a trial) was observed for the second (mean±std across trials equal to 179±45 Hz) and third (115±30 Hz) latent variables with respect to the first (69±29 Hz). Thus, we selected the 2D manifold defined by the second and third neural modes as the brain control space. The matrix mapping M1 activity into the 2D manifold was kept fixed for the rest of the experimental protocol and no other motor task session was performed.

B. BMI WITH MANIFOLD-BASED DIRECT CONTROL

Next, we tested the effectiveness and robustness of a 2D BMI with manifold-based direct control over 38 sessions (spanned over 84 days, Supp. Table I). The monkey had its arm fixed on an armrest and controlled a cursor on a screen through its M1 activity mapped into the 2D manifold (Fig. 1(b)). The second and third latent variables, hereafter referred to as L_x and L_y, were proportionally converted into the vertical (y) and horizontal (x) coordinates of the cursor, respectively. The offset of this linear relationship was adjusted across sessions to compensate for changes in baseline neural activity (see Materials and Methods). We designed a delayed point-to-point cursor control task: the animal had to first keep the cursor in a baseline position for 0.5 s and then reach and hold a target location for 0.1 s. Baseline and target locations were delimited by boxes. The distance between the baseline and target boxes was varied across sessions to promote the animal's neuromodulation ability but without demotivating her. Trial timeout was set to 8 s and successful trials were rewarded with liquid food. We employed an incremental training paradigm [20]: the number of DoFs to be controlled and the reaching space were progressively changed during the protocol (Fig. 1(c)). For the first 10 sessions, only the y-coordinate of the cursor

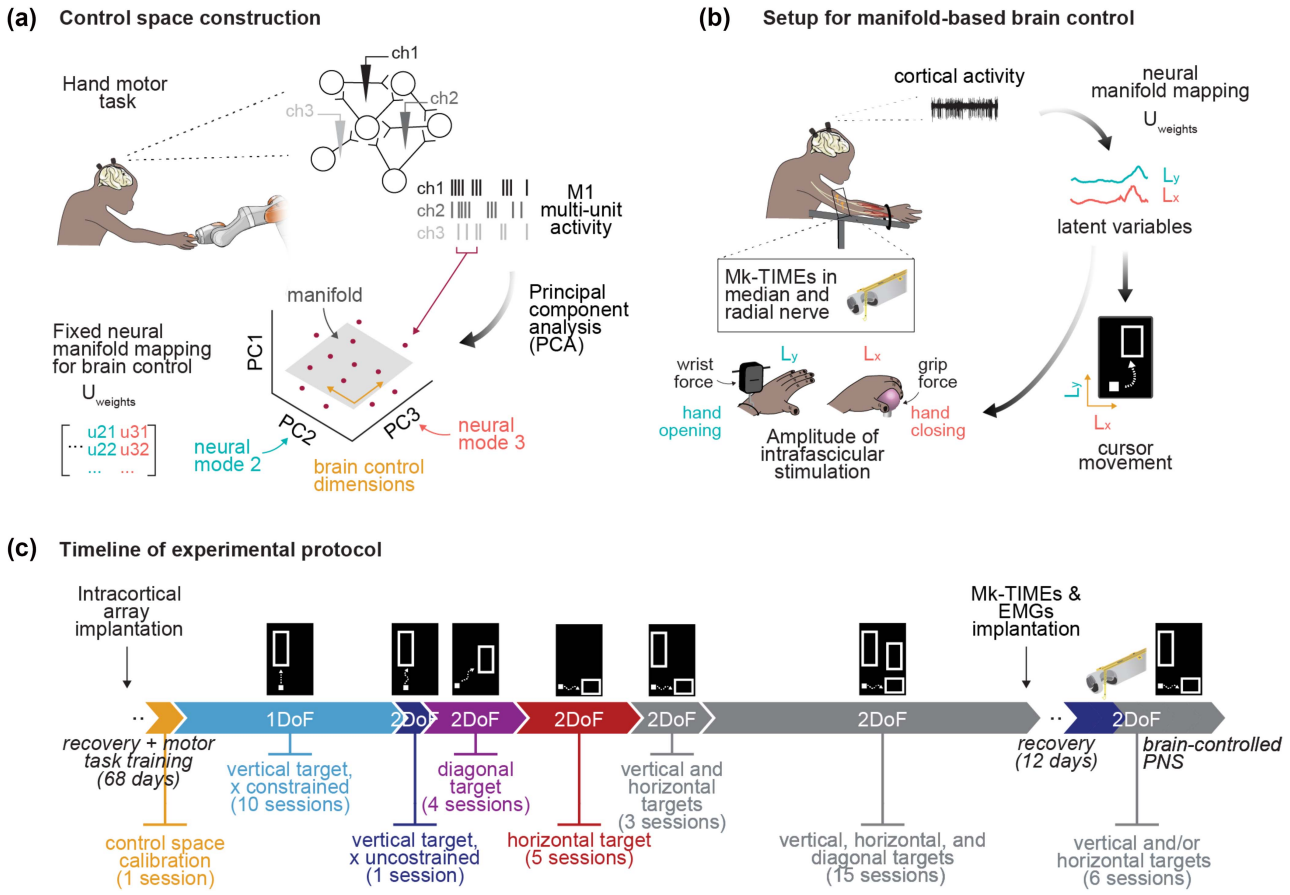

FIGURE 1. Experimental protocol for 2D manifold-based direct control. (a) Construction of the brain control space based on neural modes, illustrated in a simplified, conceptual way with three recording channels. We applied principal component analysis (PCA) to M1 multi-unit activity recorded while the animal was performing a hand motor task and evaluated the neural space defined by the three main PCs (neural modes). The firing rate of each channel at each time instant is a point (red dot) in this space. We chose the 2D manifold (grey plane) defined by the second and third neural modes (orange arrows) as the control space for subsequent brain control experiments. The $U_{weights}$ matrix contains the coefficients of the second and third PCs. (b) Setup for manifold-based direct control. The monkey had its arm fixed on an armrest and drove a cursor (white square) in 2D (orange arrows) to reach a target box (empty rectangle) by modulating its cortical activity. The cortical activity was projected in the manifold-based control space by multiplying the firing rate of M1 channels to the $U_{weights}$ matrix. The neural dynamics along the second and third neural modes (i.e., the second and third latent variables L_x and L_y), thus computed, were linearly mapped to the cursor vertical (y) and horizontal (x) coordinates, respectively. In a second phase, L_x and L_y were also linearly linked to the stimulation amplitude of two intrafascicular electrodes implanted in the radial and median nerves, respectively, to evoke hand opening and closing. (c) Timeline of experimental protocol. The different phases of brain control experiment are depicted, i.e., the number of DoFs that the monkey had to control and the position of the target to reach with the cursor.

was brain-controlled with targets placed vertically with respect to the baseline position (cyan in Fig. 1(c)): during these sessions the x-coordinate was set to 0. Next, and for the rest of the protocol, we allowed the monkey to control the cursor in both the x and y directions and we varied the location of the target: on session 11 we presented only vertical targets (blue), on sessions 12 to 15 targets were placed diagonally to the baseline position (purple), and on sessions 16 to 20, horizontally (red). Finally, between sessions 21 and 38, targets were randomly alternated (gray).

The monkey was able to effectively modulate its latent neural activity to perform the different tasks (Fig. 2(a)). The success rate was significantly above chance level ($p<0.001$, Wilcoxon signed-rank test, Fig. 2(b)), which we calculated considering latent neural activity during the intertrial periods (see Materials and Methods). Importantly, the control was possible without using hand muscle contractions (Supp. Fig. 1). The performance was high since day 1 of the first control configuration (1 DoF, vertical target), with 82% successful trials (Fig. 2(b)) which were executed in a median time of 2.41 s (Fig. 2(c)), and 21% first attempt successes (defined as the trials in which the cursor was held at the baseline and target positions for the required timespans on the first time these positions were reached, i.e., no in and out of baseline and target boxes during the trial) (Supp. Fig. 2). Over the next sessions with this configuration, we observed some small dips and rebound in the success rate, which ended at 90% on session 10 (Fig. 2(b)), a significant decrease in execution time ($p<0.001$, chi-squared test; Fig. 2(c)), and a significant increase in the percentage of trials completed on the first attempt ($p<0.01$, chi-squared test; Supp. Fig. 2). After the introduction of the horizontal DoF, the accomplishment of the vertical target task

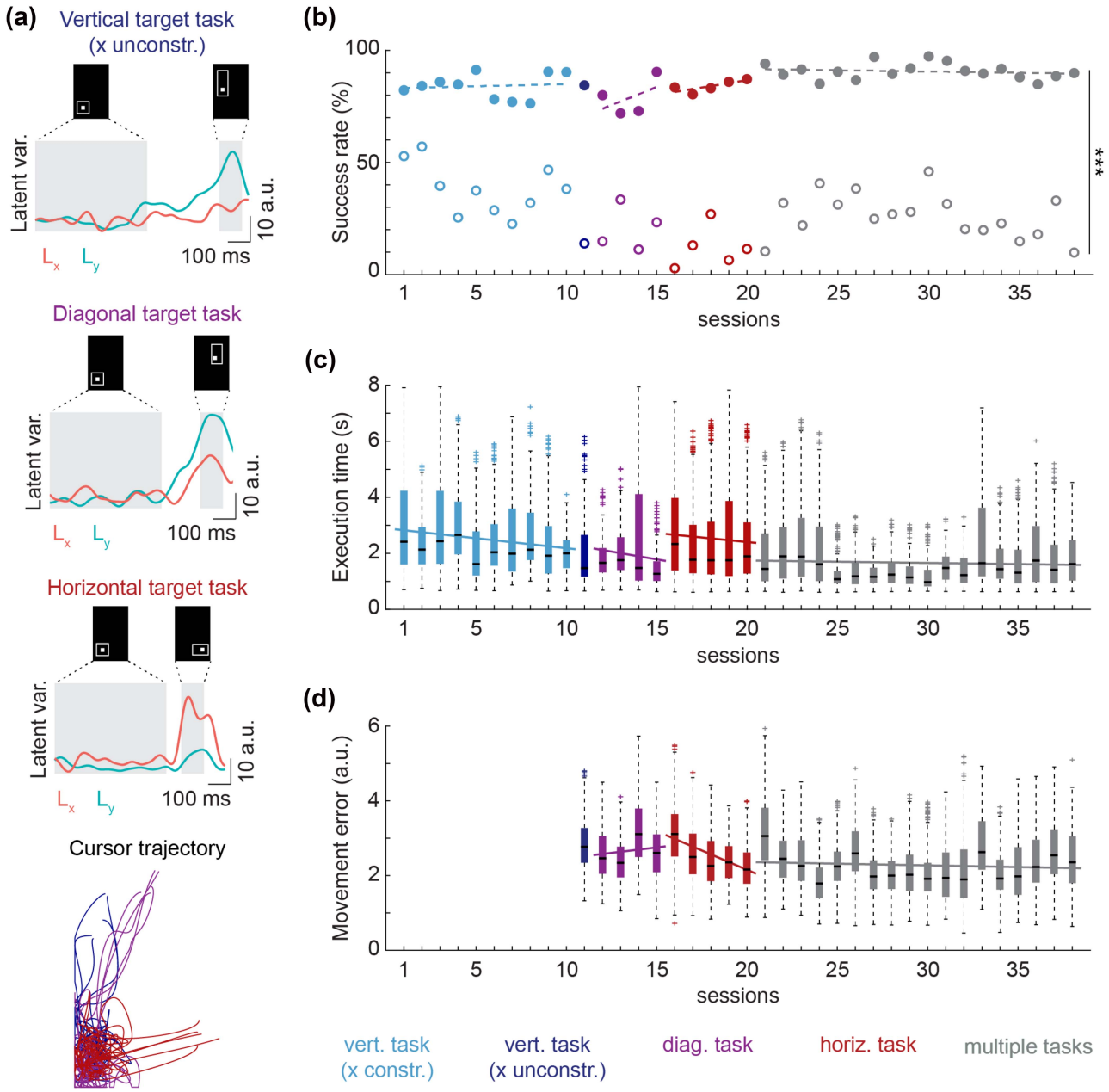

FIGURE 2. **Performance of manifold-based BMI. (a) Activation of the latent variables L_x and L_y (linearly mapped to the cursor x and y coordinates, respectively) during representative successful trials of 2D cursor control for the three types of task (vertical, horizontal, and diagonal target). The task consisted in (i) maintaining the cursor in a baseline box for 0.5 s, (ii) steering the cursor toward the target box and holding it inside it for 0.1 s. The task had to be completed within 8 s for the monkey to succeed. Bottom: cursor trajectory in representative successful trials for the three types of tasks (n = 5 per task). (b) Success rate over sessions (filled dots), together with chance performance level (empty dots) (see Materials and Methods). *** p<0.001, Wilcoxon signed-rank test. (c) Execution time of successful trials over sessions, after outliers removal. (d) Movement error (i.e., deviation of the cursor path from the ideal straight trajectory connecting the centers of the baseline and target boxes) of successful trials over sessions, after outliers removal. For the 1 DoF configuration of the first 10 sessions, the movement error could not be computed. In panels (b), (c), and (d) the different colors indicate the different types of task performed by the animal throughout the protocol. Generalized linear regression models were fitted to the data over the sessions with the same task (full line when significant, i.e., p<0.05, chi-squared test, dashed line otherwise).**

was only slightly compromised (84% successes, session 11; Fig. 2(b)). Still only a small drop in the success rate was observed when the monkey had to jointly modulate the two latent variables when the diagonal target was introduced (80% successes, session 12; Fig. 2(b)). Over the four sessions with the diagonal target, the percentage of successful trials oscillated, but reached 90% on session 15 (Fig. 2(b)); meanwhile, the execution time declined significantly (p<0.01, chi-squared test, Fig. 2(c)). When on session 16 we introduced the horizontal target, the success rate slightly decreased to 84% (Fig. 2(b)) and both the execution time (median of 2.33 s; Fig. 2(c)) and the percentage of trials completed on the first attempt (25%,

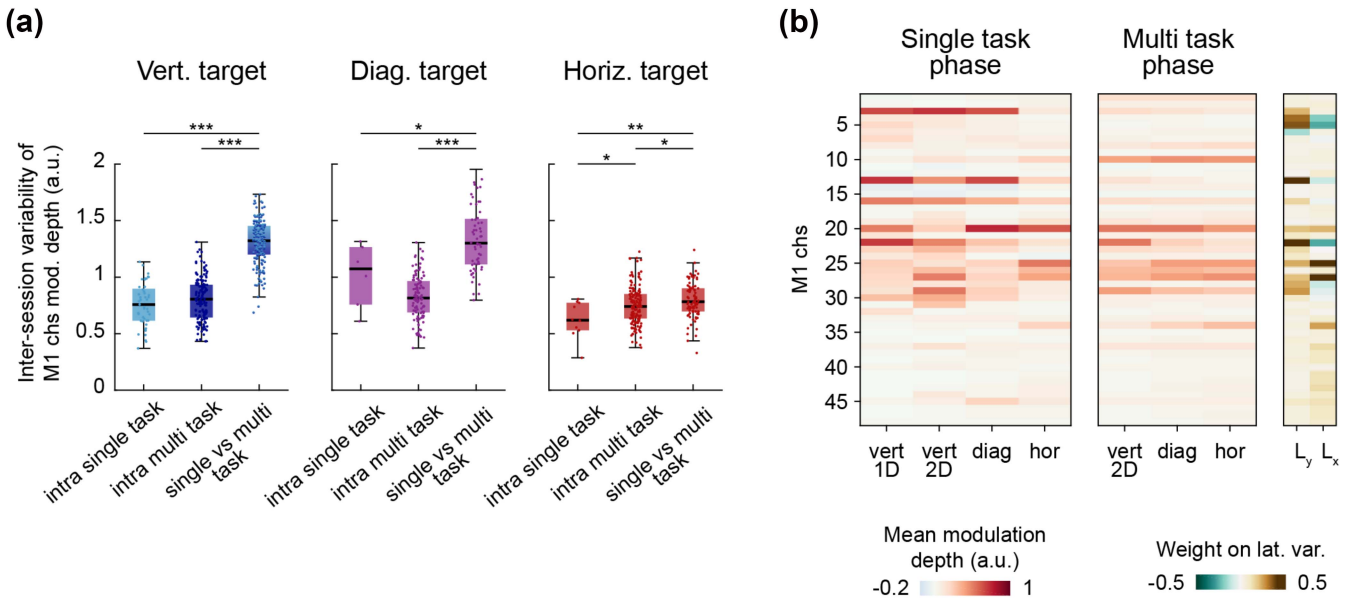

FIGURE 3. Neural tuning strategies. (a) Inter-session variability of M1 channels modulation depth within and between the two phases of the experimental protocol (i.e., single task and multi task phases) for each target type. For the vertical target, only the first 10 sessions with 1D control were considered in the single task phase, while session 11 with 2D control was excluded. (b) Normalized modulation depth of M1 channels, averaged over all trials of each protocol phase with the same target. The contribution weights of M1 channels on the two latent variables L_x and Ly are shown on the right. $*$ $p < 0.05$, $**$ $p < 0.01$, $***$ $p < 0.001$, Wilcoxon rank-sum test.

Supp. Fig. 2) returned to values close to those on the first days of the protocol. Over time, we observed an improvement in all these performance measures (Fig. 2(b)–(c), Supp. Fig. 2). After gradually adapting to the different tasks, the monkey was able to effectively switch between them. Indeed, when on session 21 we started to alternate different targets, she succeeded in 94% of the trials (Fig. 2(b)) in a median time of 1.45 s (Fig. 2(c)). The performance remained quite stable until session 38 (90% successes, Fig. 2(b); median execution time of 1.61 s, Fig. 2(c)), corresponding to 113 days after the construction of the control space (Supp. Table I).

For the 2 DoF control configurations, we measured the movement error, i.e., the average deviation of the cursor path from the ideal straight trajectory between the baseline and target positions. Because we did not impose the path to reach the target, the monkey often succeeded in the task by exploiting curved trajectories (Fig. 2(a)) due to the activation of both L_x and L_y for all the target types. The movement error remained almost constant throughout the experiment (Fig. 2(d)).

C. NEURAL TUNING STRATEGIES

During the extended timespan of the cursor control experiment, we observed day-to-day neural recording instabilities (Supp. Fig. 3), in agreement with previous studies [21], [22], [23]. We thus investigated whether, following these instabilities, the animal changed its neural tuning strategy (as measured by the modulation depth of M1 channels, see Materials and Methods) to perform the different tasks. We considered two phases of the experimental protocol: (i) when the target of interest was the only one presented (single-task phase), (ii) when it was alternated with the other targets (multi-task phase). The neural tuning strategy was variable across sessions within the same protocol phase (Supp. Fig. 4A, Fig. 3(a)), but a greater variation was observed between inter-phase sessions, especially for the vertical and diagonal targets (Fig. 3(a)). This effect can be partially explained by a larger neural turnover between inter-phase sessions due to the longer temporal gap (especially for the vertical and diagonal targets, Supp. Table 1). However, the difference in neural tuning between the two protocol phases did not increase over time or only slightly, by less than 10% (Supp. Fig. 4B), suggesting that the phase itself, and thus the circumstances of the task, also contributed to this difference.

In general, the animal used suboptimal neural tuning strategies (Fig. 3(b)). Indeed, she did preferentially modulated channels that were associated with considerable weights on the latent variables desired for the task, but also some channels that had no actual effect on the cursor, and at the same time she did not exploit channels that would have had an effect (Fig. 3(b)). This might be due to both the simplicity of the task, which did not require fine control, and the correlation between neurons. All together these results indicate that the monkey adapted its neural tuning over time led by a combination of changes in neural recordings and experimental conditions.

D. BBI WITH MANIFOLD-BASED DIRECT CONTROL

Finally, we investigated the feasibility of using our direct manifold-based brain control paradigm to drive a neuroprosthesis based on intrafascicular PNS and evoke hand movements. For this experiment, the animal was implanted with two customized intrafascicular electrodes (Mk-TIMEs)

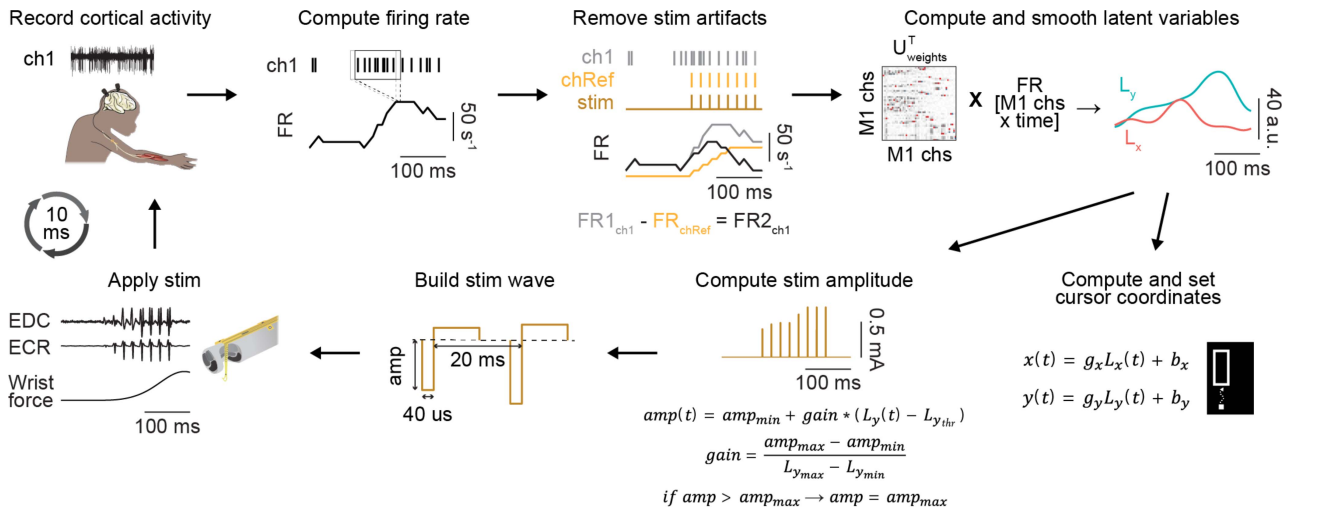

FIGURE 4. Methods for manifold-based BBI. M1 cortical activity is recorded. The firing rate of each M1 channel is computed as the number of spikes in overlapping bins of 100 ms with a sliding window of 10 ms. Stimulation artifacts are removed by subtracting the firing rate of a reference S1 channel, found to respond almost only when stimulation was applied. The latent variables L_x and L_y are computed by multiplying the firing rate of the 48 M1 channels per the $U_{weights}$ matrix. After being smoothed, L_x and L_y are linearly transformed to set the cursor x and y coordinates. The leading latent variables of the session are also linearly mapped to the amplitude of PNS (in the example, only L_y is driving stimulation). The stimulation wave is built as a train of biphasic pulses (pulse-width of 40 us, frequency of 50 Hz). Stimulation is then applied from the preselected channel (in the example of the radial Mk-TIME) thus recruiting hand muscles and generating force. The overall decoding procedure induces a time delay of approximately 10 ms.

[14], one in the median nerve and one in the radial nerve, to trigger the opening and closing of the hand, respectively. We designed the BBI experiment as follows. While the monkey, with its arm fixed, performed the cursor control task with vertical and/or horizontal targets, the latent variables L_x and L_y linearly modulated the x and y coordinates of the cursor and, from the appearance of the target box to the end of a trial, the amplitude of the stimuli applied to the median and radial nerves (Fig. 1(b)). L_x was always associated with the median nerve and L_y with the radial nerve. The animal was still rewarded when succeeding in the cursor control task.

Through a short calibration phase at the beginning of the experimental session, we set the threshold for stimulation and saturation level of the driving latent variable/s (Supp. Fig. 5A). These values were regulated to reduce target-unspecific stimuli due to the frequent coactivation of L_x and L_y, and at the same time span a large range of neuromodulation. The calibration also served to determine the functional amplitude range for the selected Mk-TIME channels (Supp. Fig. 5B), which spanned up to 0.8 mA, values consistent with our previous study on intrafascicular stimulation to evoke hand movements [14]. These parameters determined the gain and offset of the decoder translating latent neural activity into amplitude of stimulation (see Materials and Methods and Fig. 4). After setting the control parameters, we tested the BBI in triggering the two target motor functions, i.e., hand opening and closing. The full BBI protocol is described in Fig. 4. M1 activity was processed in real-time to extract spike events and compute the channels firing rate. Stimulation-induced artifacts were then removed by subtracting the firing rate of a channel of the array implanted in the somatosensory cortex (S1) that responded almost only when electrical stimuli were applied. Noise-free spike rates were projected into the 2D manifold to derive the activation of the two latent variables. After being smoothed, L_x and L_y were linearly transformed into cursor coordinates and, in addition, the leading latent variables of the session, if over the threshold, were converted into amplitude of stimulation. Charge-balanced pulses with the defined intensity were finally applied to the nerve at a frequency of 50 Hz, which we had previously found to be an adequate value for tetanized and functional muscle contractions [14]. The overall decoding procedure induced a time delay of approximately 10 ms, a value that is within the range of the cortico-muscle conduction time [21]. We repeated this experiment over 6 sessions, in which we enabled one or both types of stimulation (i.e., median, or radial) and presented to the animal one or both types of targets (i.e., vertical, or horizontal), as specified in Supp. Table II. The BBI-evoked hand movements were characterized by measuring the EMG activity of hand flexors and extensors as well as grip or wrist force (in the last two sessions).

L_x-driven median nerve stimulation effectively activated the hand flexors to close the hand when the animal accomplished the horizontal target task (Fig. 5(a) left). Conversely, L_y-driven radial nerve stimulation recruited the hand extensors to open the hand during the vertical target successes (Fig. 5(a) right). In the three sessions in which the same type of stimulation was enabled for both targets (Supp. Table II), we quantified the target specificity of the BBI. On session 39, when both types of stimulation were enabled, the specificity of median nerve stimulation for the horizontal target was 60% and the specificity of radial nerve stimulation for the vertical target was 40% (Fig. 5(b)). Results were slightly better on the two following sessions, when only a type of stimulation was enabled (Fig. 5(b)). On session 43, the specificity of median

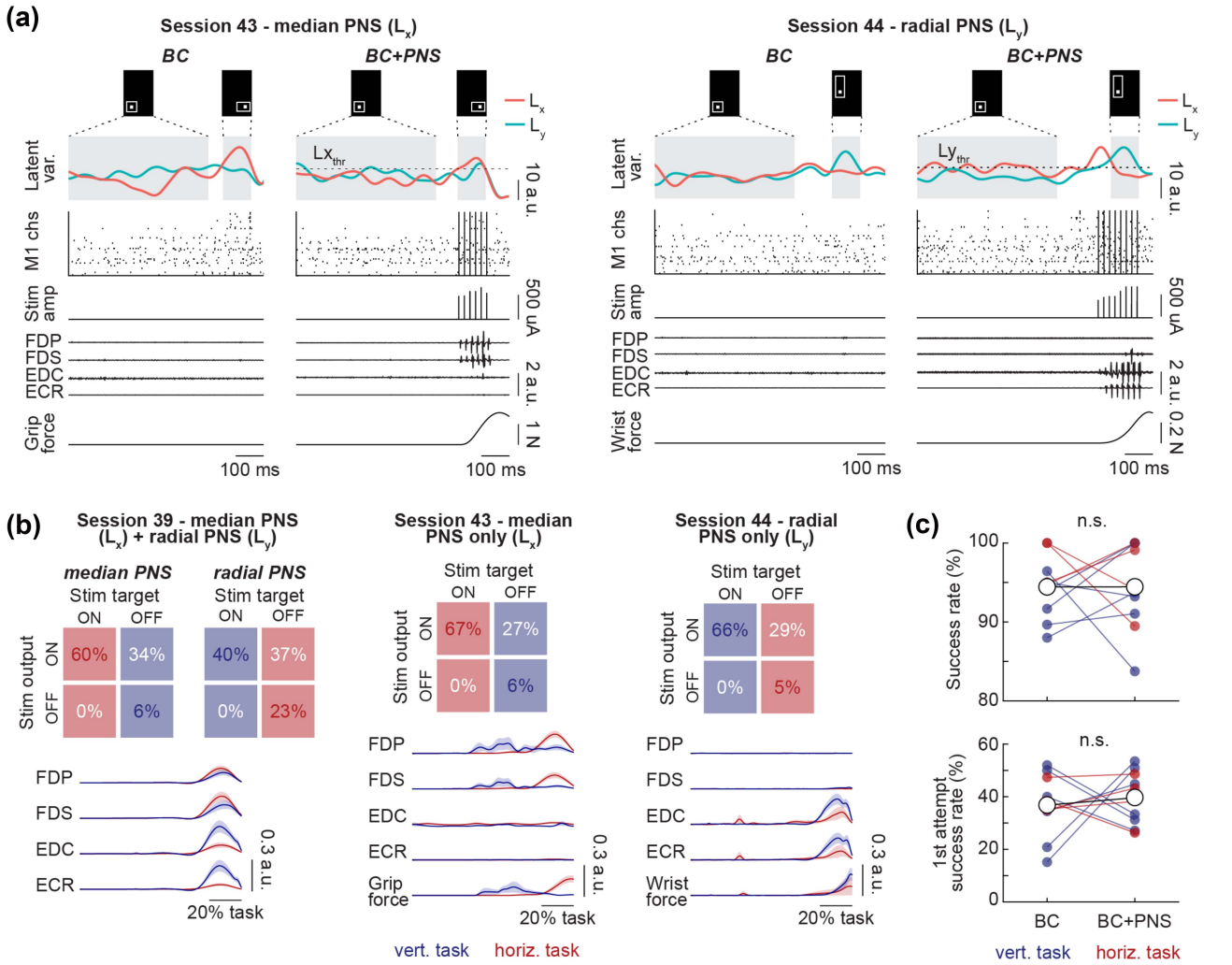

FIGURE 5. Performance of manifold-based BBI. (a) Representative successful trials of brain cursor control task when PNS was enabled or was not enabled (i.e., calibration trials, see Materials and Methods) from two sessions of brain PNS control. In both cases, the monkey performed the cursor control task (and received a reward when succeeding in this task), but when PNS was enabled, the latent variables controlled both the movement of the cursor and the amplitude of PNS. On session 43, L_x was linearly mapped to median nerve stimulation to recruit flexor muscles and close the hand. On session 44, L_y was linearly mapped to radial nerve stimulation to recruit extensor muscles and open the hand. Stimulation was enabled only after succeeding in the baseline phase of the cursor control task and activated when the leading latent variable exceeded the threshold. (b) Quantification of the target specificity of the BBI (PNS enabled) on session 39 (both median and radial nerve stimulation enabled, controlled by L_x and L_y, respectively), on session 43 (only median nerve stimulation enabled, controlled by L_x), and on session 44 (only radial nerve stimulation enabled, controlled by L_y). Top for each session: confusion matrices showing the percentage of successful trials in which stimulation was activated or kept off as desired or not (i.e., median nerve stimulation, which was controlled by L_x, should ideally have been delivered for the horizontal target and kept off for the vertical target, whereas radial nerve stimulation, which was controlled by L_y, should ideally have been delivered for the vertical target and kept off for the horizontal target). Bottom for each session: hand muscle activity and force (for sessions 43 and 44), generated by stimulation, averaged across all successful trials with the same target type (vertical and horizontal). (c) Comparison of success rate in the brain cursor control task when PNS was enabled or was not enabled (calibration trials, see Materials and Methods) (n = 10, 6 sessions). Data referring to the same session and the same target type (vertical or horizontal) were pairwise compared. On the 6 sessions, median nerve stimulation was modulated by L_x, whereas radial nerve stimulation was modulated by L_y. Except on the first session, only one type of stimulation was enabled at a time (Supp. Table II). n.s. = not significant ($p>0.05$, Wilcoxon signed-rank test). Abbreviations: flexor digitorum profundus (FDP), flexor digitorum superficialis (FDS), extensor digitorum communis (EDC), extensor carpi radialis (ECR).

nerve stimulation for the horizontal target was 67%, whereas on session 44, the specificity of radial nerve stimulation for the horizontal target was 66%. Overall, many spurious stimuli were delivered, even though the undesired motor responses had a minor strength compared to those desired (Fig. 5(b)).

We next controlled whether PNS perturbed the brain cursor control task. Indeed, almost every electrical stimulus evoked an artifact in all M1 channels (Supp. Fig. 6A), and artifacts were stronger as the amplitude of stimulation increased (Supp. Fig. 6B). Through postprocessing, we found that the reference S1 channel was also almost always triggered by stimulation (Supp. Fig. 6A) and only few spontaneous spikes were detected on it (Supp. Fig. 6C), confirming that the channel choice was adequate. Considering all six sessions,

we did not observe a significant decrease in either the success rate ($p = 0.38$, Wilcoxon signed-rank test) nor the percentage of trials completed on the first attempt ($p = 0.25$, Wilcoxon signed-rank test) compared with the PNS-free setting (based on the calibration trials) (Fig. 5(c)), confirming the efficacy of our procedure for stimulation artifacts removal.

III. DISCUSSION

We preliminarily investigated in a monkey the feasibility of a 2-DoF brain control strategy confined within a fixed intrinsic motor manifold [15] for a BBI application. Our brain decoding module was based on the direct linear coupling between latent neural dynamics and output commands. We aimed at analyzing the ease of learning and long-term performance of this control strategy as well as the possibility of integrating it with intrafascicular PNS.

First, we assessed the within-manifold neuromodulation ability of the monkey in a simple 2D delayed point-to-point cursor control task with incremental variations. This BMI paradigm provided us with the flexibility necessary to study the long-term temporal and task-related effects on the animal's performance. With only day-to-day adjustments of decoding scale factors, our brain control strategy was easy-to-learn and robust. The animal showed a high success rate from the first day of the experiment without prior training and adapted readily to new tasks. We did observe small drops in proficiency when a change in neuromodulation strategy was required, but these were easily compensated for with little practice. This result was certainly favored by the simplicity of the task but is also likely due to the incremental design of the training protocol [20] and the "ecological" BMI mapping employed. By fixing the control space within an intrinsic manifold, we exploited natural (i.e., already acquired) neural activity patterns [17], and by intuitively relating the cursor movement to these patterns, we facilitated learnability. We add that while we changed the number of DoFs and the task when we qualitatively observed a sufficient improvement in the animal's performance, it would have been interesting to study the different control conditions for the same number of sessions to compare their learning rate.

The monkey was then able to consistently switch between the different tasks, maintaining a success rate of ∼90% until the end of the protocol (113 days after the control space construction, Supp. Table I). This long-term robustness is promising, as neural recording instabilities in chronic settings constitute one of the main challenges for the clinical translation of BMIs [22], [23], [24]. As mentioned earlier, decoding parameters had to be adapted daily for this result. However, these included only the gain and offset of the linear conversion of latent neural activity into output variables, which were determined by performing a few trials of cursor control task, i.e., ∼15-20 trials (see Materials and Methods), at the beginning of each session. In a clinical setting, this procedure could be performed quickly and automatically, also considering that the number of calibration trials we used is not the lower limit and could be further reduced. Moreover, since the calibration factors were applied equally to all M1 channels, there was no compensation for neural turnover. For the same reason, our recalibration does not coincide with the recalculation of the motor manifold, i.e., the contribution weights of the M1 channels on the neural modes, which would also have been more laborious and time-consuming, i.e., 15-20 cursor control trials to compute our decoding parameters compared to about 100 motor trials to recompute the manifold [18]. In our scenario, the monkey had to adjust neural tuning over time to preserve performance, which she did in a way that also depended on the experimental conditions. We believe that this effortless adaptation is still due to the inherence of manifold-based control [17] and the stability of latent dynamics [18], in addition to the simplicity of the task and the incremental training. These results showing neural adaptability to a fixed control space expand previous findings on the potential of neural plasticity for BMI applications [25], [26].

As a final step, we conducted a pilot experiment to test our direct manifold-based control strategy in driving a PNS-based neuroprosthesis for hand opening and closing. By training the monkey to timely up-regulate latent neural activity that linearly modulated the amplitude of intrafascicular PNS, our approach enabled the timely triggering of hand movements. Importantly, although it certainly elicited sensory percepts [27], stimulation did not impair performance in cursor control. These proof-of-concept results demonstrate the feasibility of integrating our decoding paradigm into a BBI.

A limitation of this study was the simplicity of the point-point cursor control task, which included only three targets and lacked constraints on the cursor trajectory. As mentioned above, this likely contributed to the success rate being high since the very first sessions. Another related limitation was the limited accuracy in effector control. Since our training paradigm lacked instructions that encouraged straight cursor trajectories, it did not favor accuracy. The monkey frequently reached the visual target along curved cursor paths due to activation of both latent variables. This led, in the BBI phase, to the target-unspecific application of stimuli to the median and radial nerves, inducing weaker but frequent undesired muscle responses. In view of applying this control strategy to motor functions that require the coordinated recruitment of hand flexors and extensors, a more constrained task, such as an instructed-path [28] or pursuit-tracking [29] task, should be used in the future to promote independent and finer control of the latent variables. This scenario would also be crucial to challenge the ease of learning of manifold-based decoding and investigate whether it can achieve the level of control accuracy and smoothness provided by state-of-the-art algorithms such as the Kalman filter [30], [31]. Moreover, while we have limited our BBI paradigm to the control of two motor DoFs, extending it to more complex movements will require additional control signals. In this framework, it will become increasingly critical to ensure the decoupling of latent neural dynamics to separately control multiple stimulation channels targeting specific muscles or muscle synergies. Finally, further

validation with a larger number of monkeys is necessary to generalize our results.

In the perspective of clinical translation to people with motor disabilities, some practical points need to be discussed. First, the efficacy of a manifold identification method based on imagined or attempted movements has yet to be validated. However, since M1 was shown to be amply engaged not only in overt movements but also in cognitive motor processes [32], we believe that goal-directed motor imagery or motor attempt would be effective construction paradigms, as usual in BMI and BBI clinical applications [33]. We also point out that brain areas such as premotor or parietal cortices could provide an interesting alternative or complement to M1 to derive intrinsic low-dimensional spaces associated with motor control [15], [34]. Second, the choice of the motor tasks may be critical for the ease-of-learning of the BBI. Here, the neural manifold was identified based on a center-out reaching movement which was structurally related to the point-to-point cursor motion. Although experimental verification of this point is lacking, our recommendation would be to select motor tasks that are congruent with the final BBI task. In the same line, we note that a larger repertoire of movements may be necessary for more complex control. Third, while this approach is more directly applicable to patients suffering from motor disorders that do not affect the cerebral cortex, such as spinal cord injury or brainstem stroke, neural tuning adaptability after cortical injuries remains to be tested. Since it was shown that cortical stroke survivors can learn to modulate ipsilesional cortical rhythms [35], we believe that control of latent neural dynamics is also possible and could be enhanced by brain stimulation [35]. Moreover, studies have shown that BBIs can promote neurological recovery [35], [36], [37], [38], [39], [40] thanks to the contingent link between brain activity and body mobilization which triggers Hebbian-like plasticity [41]. Therefore, we believe that our BBI would act like a reinforcing loop that simultaneously exploits and promotes neural plasticity. Fourth and finally, clinical experiments are needed to confirm that the sensations inevitably elicited by stimulation of mixed nerves do not impair the patients' mastery of control, as was the case here with the animal. This might also depend on the patient's clinical picture. In general, we expect that people with neurological diseases such as stroke and spinal cord injury will tolerate the evoked sensations because they often have sensory deficits in addition to motor deficits, and furthermore, intrafascicular stimuli of similar intensity did not provoke discomfort even when they were specifically used to activate sensory fibers in amputees [27]. However, some of these patients might suffer from hyperalgesia or allodynia [42], [43]. Moreover, it should be verified that the sensations perceived, even if tolerable, are not distracting or obstructive to the control. All this requires clinical testing.

IV. CONCLUSION

We conclude that direct control based on latent neural dynamics is a feasible paradigm for BBI applications with promising characteristics in terms of intuitiveness and reliability, resulting from the inherence of neural manifolds and the simplicity of direct control links. These demonstrations constitute an important steppingstone for human studies of brain-controlled PNS.

V. MATERIALS AND METHODS

We performed experiments in a macaque monkey implanted with a Utah array in M1 and Mk-TIMEs in the median and radial nerves. We computed a 2D motor neural manifold by applying PCA to M1 activity recorded in a session when the animal performed a reach-and-grasp-task. We then used M1 activity projected along manifold axes to proportionally control the 2D coordinates of a computer cursor. We tested this BCI paradigm in a point-to-point task with incremental variations over more than three months. Finally, we additionally coupled latent neural activity to the amplitude of median and radial nerve stimulation to evoke voluntary hand movements. Details are specified in Supplementary Methods.

SUPPLEMENTARY MATERIALS

Supplementary material contains a detailed description of the methods alongside with supplementary figures and tables.

COMPETING INTERESTS

EL, SS, and SM are founders of Action Potential Neurotechnology, a company that develops implantable neuroprostheses. The remaining authors declare no competing interests.

AUTHOR CONTRIBUTIONS

SM, AB, and MB conceived the study. SM acquired funding. MB and AB designed and implemented the experimental setup. MB, ER, MD, and EL conducted the experiments. EL, MB, and ER analyzed the data. SM and SS supervised the study. EL and MB prepared the figures. EL, MB, and SS wrote the manuscript. All authors reviewed the manuscript.

ACKNOWLEDGMENT

The authors would like to thank Prof. Eric M. Rouiller and Dr. Marco Capogrosso for helpful advice and discussions; Dr. Sophie Wurth and Dr. Simon Borgognon for help with the experiments; J. Maillard and L. Bossy for the care provided to the monkey; A. Zbinden for the veterinary survey of the animal.

REFERENCES

[1] J. L. Collinger, M. L. Boninger, T. M. Bruns, K. Curley, W. Wang, and D. J. Weber, "Functional priorities, assistive technology, and brain-computer interfaces after spinal cord injury," *J. Rehabil. Res. Develop.*, vol. 50, pp. 145–160, 2013, doi: 10.1682/jrrd.2011.11.0213.

[2] L. R. Hochberg et al., "Reach and grasp by people with tetraplegia using a neurally controlled robotic arm," *Nature*, vol. 485, pp. 372–375, 2012, doi: 10.1038/nature11076.

[3] C. T. Moritz, S. I. Perlmutter, and E. E. Fetz, "Direct control of paralysed muscles by cortical neurons," *Nature*, vol. 456, pp. 639–642, 2008, doi: 10.1038/nature07418.

[4] E. A. Pohlmeyer et al., "Toward the restoration of hand use to a paralyzed monkey: Brain-controlled functional electrical stimulation of forearm muscles," *PLoS one*, vol. 4, 2009, Art. no. e5924, doi: 10.1371/journal.pone.0005924.

[5] C. Ethier, E. R. Oby, M. J. Bauman, and L. E. Miller, "Restoration of grasp following paralysis through brain-controlled stimulation of muscles," *Nature*, vol. 485, no. 7398, pp. 368–371, 2012, doi: 10.1038/nature10987.

[6] M. Capogrosso et al., "A brain–spine interface alleviating gait deficits after spinal cord injury in primates," *Nature*, vol. 539, pp. 284–288, 2016, doi: 10.1038/nature20118.

[7] B. Barra et al., "Epidural electrical stimulation of the cervical dorsal roots restores voluntary upper limb control in paralyzed monkeys," *Nature Neurosci.*, vol. 25, pp. 924–934, 2022, doi: 10.1038/s41593-022-01106-5.

[8] C. E. Bouton et al., "Restoring cortical control of functional movement in a human with quadriplegia," *Nature*, vol. 533, pp. 247–250, 2016, doi: 10.1038/nature17435.

[9] A. B. Ajiboye et al., "Restoration of reaching and grasping movements through brain-controlled muscle stimulation in a person with tetraplegia: A proof-of-concept demonstration," *Lancet*, vol. 389, pp. 1821–1830, 2017, doi: 10.1016/S0140-6736(17)30601-3.

[10] S. C. I. Colachis et al., "Dexterous control of seven functional hand movements using cortically-controlled transcutaneous muscle stimulation in a person with tetraplegia," *Front. Neurosci.*, vol. 12, 2018, Art. no. 313435, doi: 10.3389/fnins.2018.00208.

[11] G. Pfurtscheller, G. R. Müller, J. Pfurtscheller, H. J. Gerner, and R. Rupp, "'Thought'– Control of functional electrical stimulation to restore hand grasp in a patient with tetraplegia," *Neurosci. Lett.*, vol. 351, pp. 33–36, 2003, doi: 10.1016/S0304-3940(03)00947-9.

[12] C. E. King, P. T. Wang, C. M. McCrimmon, C. C. Chou, A. H. Do, and Z. Nenadic, "The feasibility of a brain-computer interface functional electrical stimulation system for the restoration of overground walking after paraplegia," *J. NeuroEngineering Rehabil.*, vol. 12, 2015, Art. no. 80, doi: 10.1186/s12984-015-0068-7.

[13] S. Shokur, A. Mazzoni, G. Schiavone, D. J. Weber, and S. Micera, "A modular strategy for next-generation upper-limb sensory-motor neuroprostheses," *Med*, vol. 2, pp. 912–937, 2021, doi: 10.1016/j.medj.2021.05.002.

[14] M. Badi et al., "Intrafascicular peripheral nerve stimulation produces fine functional hand movements in primates," *Sci. Transl. Med.*, vol. 13, 2021, Art. no. eabg6463, doi: 10.1126/scitranslmed.abg6463.

[15] J. A. Gallego, M. G. Perich, L. E. Miller, and S. A. Solla, "Neural manifolds for the control of movement," *Neuron*, vol. 94, pp. 978–984, 2017, doi: 10.1016/j.neuron.2017.05.025.

[16] G. F. Elsayed and J. P. Cunningham, "Structure in neural population recordings: An expected byproduct of simpler phenomena?," *Nature Neurosci.*, vol. 20, pp. 1310–1318, 2017, doi: 10.1038/nn.4617.

[17] P. T. Sadtler et al., "Neural constraints on learning," *Nature*, vol. 512, pp. 423–426, 2014, doi: 10.1038/nature13665.

[18] J. A. Gallego, M. G. Perich, R. H. Chowdhury, S. A. Solla, and L. E. Miller, "Long-term stability of cortical population dynamics underlying consistent behavior," *Nature Neurosci.*, vol. 23, pp. 260–270, 2020, doi: 10.1038/s41593-019-0555-4.

[19] B. Barra et al., "A versatile robotic platform for the design of natural, three-dimensional reaching and grasping tasks in monkeys," *J. Neural Eng.*, vol. 17, 2019, Art. no. 016004, doi: 10.1088/1741-2552/ab4c77.

[20] E. R. Oby et al., "New neural activity patterns emerge with long-term learning," *Proc. Nat. Acad. Sci.*, vol. 116, pp. 15210–15215, 2019, doi: 10.1073/pnas.1820296116.

[21] G. M. Van Acker III, C. W. Luchies, and P. D. Cheney, "Timing of cortico-muscle transmission during active movement," *Cereb. Cortex*, vol. 26, pp. 3335–3344, 2016, doi: 10.1093/cercor/bhv151.

[22] A. S. Dickey, A. Suminski, Y. Amit, and N. G. Hatsopoulos, "Single-unit stability using chronically implanted multielectrode arrays," *J. Neurophysiol.*, vol. 102, pp. 1331–1339, 2009, doi: 10.1152/jn.90920.2008.

[23] R. D. Flint, M. R. Scheid, Z. A. Wright, S. A. Solla, and M. W. Slutzky, "Long-term stability of motor cortical activity: Implications for brain machine interfaces and optimal feedback control," *J. Neurosci.*, vol. 36, pp. 3623–3632, 2016, doi: 10.1523/JNEUROSCI.2339-15.2016.

[24] J. E. Downey, N. Schwed, S. M. Chase, A. B. Schwartz, and J. L. Collinger, "Intracortical recording stability in human brain–computer interface users," *J. Neural Eng.*, vol. 15, 2018, Art. no. 046016, doi: 10.1088/1741-2552/aab7a0.

[25] K. Ganguly and J. M. Carmena, "Emergence of a stable cortical map for neuroprosthetic control," *PLoS Biol*, vol. 7, 2009, Art. no. e1000153, doi: 10.1371/journal.pbio.1000153.

[26] A. L. Orsborn, H. G. Moorman, S. A. Overduin, M. M. Shanechi, D. F. Dimitrov, and J. M. Carmena, "Closed-loop decoder adaptation shapes neural plasticity for skillful neuroprosthetic control," *Neuron*, vol. 82, pp. 1380–1393, 2014, doi: 10.1016/j.neuron.2014.04.048.

[27] S. Raspopovic et al., "Restoring natural sensory feedback in real-time bidirectional hand prostheses," *Sci. Transl. Med.*, vol. 6, 2014, Art. no. 222ra19, doi: 10.1126/scitranslmed.3006820.

[28] P. T. Sadtler, S. I. Ryu, E. C. Tyler-Kabara, B. M. Yu, and A. P. Batista, "Brain–computer interface control along instructed paths," *J. Neural Eng.*, vol. 12, 2015, Art. no. 016015, doi: 10.1088/1741-2560/12/1/016015.

[29] L. R. Hochberg et al., "Neuronal ensemble control of prosthetic devices by a human with tetraplegia," *Nature*, vol. 442, pp. 164–171, 2006, doi: 10.1038/nature04970.

[30] S.-P. Kim, J. D. Simeral, L. R. Hochberg, J. P. Donoghue, and M. J. Black, "Neural control of computer cursor velocity by decoding motor cortical spiking activity in humans with tetraplegia," *J. Neural Eng.*, vol. 5, pp. 455–476, 2008, doi: 10.1088/1741-2560/5/4/010.

[31] S.-P. Kim, J. D. Simeral, L. R. Hochberg, J. P. Donoghue, G. M. Friehs, and M. J. Black, "Point-and-click cursor control with an intracortical neural interface system by humans with tetraplegia," *IEEE Trans. Neural Syst. Rehabil. Eng.*, vol. 19, no. 2, pp. 193–203, Apr. 2011, doi: 10.1109/TNSRE.2011.2107750.

[32] C. E. Vargas-Irwin et al., "Watch, imagine, attempt: Motor cortex single-unit activity reveals context-dependent movement encoding in humans with tetraplegia," *Front. Hum. Neurosci.*, vol. 12, 2018, Art. no. 450, [Online]. Available: https://www.frontiersin.org/article/10.3389/fnhum.2018.00450

[33] N. G. Hatsopoulos and A. J. Suminski, "Sensing with the motor cortex," *Neuron*, vol. 72, pp. 477–487, 2011, doi: 10.1016/j.neuron.2011.10.020.

[34] J. A. Gallego, T. R. Makin, and S. D. McDougle, "Going beyond primary motor cortex to improve brain–computer interfaces," *Trends Neurosci.*, vol. 45, pp. 176–183, 2022, doi: 10.1016/j.tins.2021.12.006.

[35] S. R. Soekadar, N. Birbaumer, M. W. Slutzky, and L. G. Cohen, "Brain–machine interfaces in neurorehabilitation of stroke," *Neurobiol. Dis.*, vol. 83, pp. 172–179, 2015, doi: 10.1016/j.nbd.2014.11.025.

[36] J. J. Daly, R. Cheng, J. Rogers, K. Litinas, K. Hrovat, and M. Dohring, "Feasibility of a new application of noninvasive brain computer interface (BCI): A case study of training for recovery of volitional motor control after stroke," *J. Neurologic Phys. Ther.*, vol. 33, pp. 203–211, 2009, doi: 10.1097/NPT.0b013e3181c1fc0b.

[37] A. Biasiucci et al., "Brain-actuated functional electrical stimulation elicits lasting arm motor recovery after stroke," *Nature Commun.*, vol. 9, 2018, Art. no. 2421, doi: 10.1038/s41467-018-04673-z.

[38] M. Bonizzato et al., "Brain-controlled modulation of spinal circuits improves recovery from spinal cord injury," *Nature Commun.*, vol. 9, 2018, Art. no. 3015, doi: 10.1038/s41467-018-05282-6.

[39] J. G. McPherson, R. R. Miller, and S. I. Perlmutter, "Targeted, activity-dependent spinal stimulation produces long-lasting motor recovery in chronic cervical spinal cord injury," *Proc. Nat. Acad. Sci.*, vol. 112, pp. 12193–12198, 2015, doi: 10.1073/pnas.1505383112.

[40] A. Selfslagh et al., "Non-invasive, brain-controlled functional electrical stimulation for locomotion rehabilitation in individuals with paraplegia," *Sci. Rep.*, vol. 9, 2019, Art. no. 6782, doi: 10.1038/s41598-019-43041-9.

[41] C. Ethier and L. E. Miller, "Brain-controlled muscle stimulation for the restoration of motor function," *Neurobiol. Dis.*, vol. 83, pp. 180–190, 2015, doi: 10.1016/j.nbd.2014.10.014.

[42] R. A. Harrison and T. S. Field, "Post stroke pain: Identification, assessment, and therapy," *Cerebrovascular Dis.*, vol. 39, pp. 190–201, 2015, doi: 10.1159/000375397.

[43] E. M. Hagen and T. Rekand, "Management of neuropathic pain associated with spinal cord injury," *Pain Ther.*, vol. 4, pp. 51–65, 2015, doi: 10.1007/s40122-015-0033-y.